Chemical Engineering Journal 485 (2024) 149982

Contents lists available at ScienceDirect

Chemical Engineering Journal

journal homepage: www.elsevier.com/locate/cej

Techno-economic analysis of onboard CO_2 capture for ultra-large container ships

Marco Visonà, Fabrizio Bezzo, Federico d'Amore *

CAPE-Lab – Computer-Aided Process Engineering Laboratory, Department of Industrial Engineering, University of Padova, via Marzolo 9, PD, Padova, 35131, Italy

ARTICLE INFO

Keywords:
Onboard carbon capture
Ship sector decarbonisation
Ultra-large container ship
Techno-economic analysis
Electric heat pump

ABSTRACT

Decarbonising the naval shipping sector is of paramount importance to decrease global CO_2 emissions. This work presents a techno-economic analysis of onboard solvent-based carbon capture for an ultra-large container ship, powered by two dual-fuel engines fed with either heavy fuel oil or liquefied natural gas. Different case studies are proposed depending on the fuel used by the ship and on the chosen design to supply the necessary heat and electricity to the carbon capture unit. Aside a conventional strategy based on heat provided via fuel combustion in a boiler, a novel configuration based on electric heat pump is investigated. The economic analysis is based on a real inter-continental journey. The results highlight that onboard carbon capture determines an increase in fuel consumption with respect to the unabated ship, that varies depending on the exhaust gas CO_2 content (hence, on the ship fuel) and on the selected process design. The integration of the electric heat pump leads to a significant decrease in this additional fuel consumption and better results in terms of CO_2 avoidance and costs. The carbon abatement cost is found in the range of 64–149 €/t of CO_2 avoided.

1. Introduction

Naval shipping is a fundamental artery of international commerce as it handles more than 80% of world trade by volume. However, this sector poses significant challenges due to its substantial greenhouse gases (GHGs) emissions, particularly carbon dioxide (CO_2). In 2022, the naval shipping sector emitted 706 Mt of CO_2, which corresponds to about 2% of global emissions [1]. Moreover, as the maritime trade is expected to increase over the medium term at a +2.1% yearly pace [2], so will do its expected emissions if no abatement measures are implemented. In this respect, the international maritime organisation (IMO) predicted a significant increase in naval sector emissions by 2050 against the 2008 level [3]. Recently, this organisation set the goal to peak GHG emissions from international shipping [4], by adopting different measures: (*i*) increasing the efficiency of ships (e.g., speed reduction, better design of hull parameters, propulsion, route, and trim optimisation); (*ii*) switching to low-carbon alternative fuels, such as ammonia [5], liquefied natural gas [6], biofuels, hydrogen [7], and electro-Fuels (e-Fuels) like e-Methanol [8]; and (*iii*) adopting onboard carbon capture. While increases in ship efficiencies are desirable, these are inherently not sufficient to meet the goal of net zero emissions. On the other hand, a fuel switch requires the establishment of novel infrastructures and new ships, and is accordingly perceived as an attractive option in a long-term perspective [9]. Differently, onboard carbon capture, which is the focus of this study, may represent a short-to-medium term alternative. It consists in separating the CO_2 from the flue gases of the ship, which is then liquefied for onboard storage in tanks, before unloading at ports. As such, onboard carbon capture could be a complementary and additional tool for shipbuilders to comply with regulations and meet future net zero targets [10]. Moreover, it could be a bridging technology to reduce the emission intensity of current vessels. This work proposes the techno-economic design of a solvent-based, post-combustion, onboard carbon capture plant for an ultra-large container vessel, operating between East Asia and North Europe. This technology is chosen due to its high level of maturity and retrofitability. However, it should be highlighted that more advanced capture configurations, though currently characterised by a lower technology readiness level, may lead to a better techno-economic performance [11–14].

One challenge for the design of carbon capture systems onboard ships is how to provide the energy (mainly in the form of heat, but also electricity) that is required to operate the carbon capture unit, particularly for solvent regeneration in the case of post-combustion capture. On this line, one of the first studies was published by Luo and Wang [15], based on a heavy fuel oil (HFO) fuelled cargo ship with a dead-weight of 12500 t and powered by two engines providing 17 MW of nominal power output. They obtained a carbon capture rate of

* Corresponding author.
E-mail address: federico.damore@unipd.it (F. d'Amore).

https://doi.org/10.1016/j.cej.2024.149982
Received 5 December 2023; Received in revised form 16 February 2024; Accepted 23 February 2024
Available online 24 February 2024
1385-8947/

Acronyms

Case FB	Case study with fuel boiler integration
Case FG	Case study with flue gas heat integration
Case HP	Case study with electric heat pump integration
CEPCI	Chemical engineering plant cost index
COP	Coefficient of performance
DWT	Dead-weight
EGR	Exhaust gas recirculation
FEU	Forty foot equivalent unit container
GHG	Greenhouse gas
HFO	Heavy fuel oil
IMO	International maritime organisation
LHV	Lower heating value
LNG	Liquefied natural gas
MEA	Monoethanolamine
S1	Unloading Scenario 1
S2	Unloading Scenario 2
S3	Unloading Scenario 3
TEU	Twenty foot equivalent unit container

Mathematical symbols

a	Parameter for equipment purchase price [€]
b	Coefficient for equipment purchase price [€/relevant unit]
C	Equipment purchase price [€]
$CAPEX$	Capital expenditure [M€]
$CAPEX_y$	Annualised capital expenditure [M€/y]
C_{cargo}	Annual reduced transport capacity cost [M€/y]
C_{fuel}	Annual fuel cost [M€/y]
C_{MEA}	Annual solvent cost [M€/y]
$C_{T\&S}$	Annual unloading cost [M€/y]
$\Delta m_{cargo,k}$	Variation in mass of commercial cargo for leg k [t]
d_k	Duration of leg k [days]
d_{tot}	Total voyage duration [days]
DWT_k	Dead-weight for leg k [t]
η_{boiler}	Fuel boiler thermal efficiency [%]
η_{engine}	Ship engine electric efficiency [%]
f	Installation factor
FCI	Fixed capital investment [M€]
$fOPEX$	Fixed operational expenditure [M€/y]
fr	Freight rate [FEU]
i	Interest rate [%]
$ISBL$	Inside battery limits plant costs [M€]
$LHV_{i,j}$	Lower heating value of fuel i for unit j [MJ/kg]
$m_{cargo,k}$	Mass of commercial cargo for leg k [t]
$m_{CO_2,k}$	Mass of CO_2 stored onboard for leg k [t]
$\dot{m}_{fuel}$	Excess fuel mass flow rate [kg/s]
$\hat{m}_{fuel}$	Yearly excess fuel consumption [t/y]
$m_{fuel,k}$	Mass of fuel loaded for leg k [t]
$\hat{m}_{MEA}$	Yearly solvent consumption [t/y]
n	Scaling exponential factor for equipment purchase price [–]
$OSBL$	Outside battery limits plant costs [M€]
$\dot{Q}_{available}$	Thermal power from flue gas heat integration [MW_{th}]
$\dot{Q}_{reb}$	Capture unit reboiler duty [MW_{th}]
S	Scaling size for equipment purchase price [relevant unit]
t	Plant lifetime [years]
TAC	Total annual cost [M€/y]
$vOPEX$	Variable operational expenditure [M€/y]
$\dot{W}_{comp}$	Compressor(s) power demand [MW_{el}]

73%–90% thanks to the flue gas available at a relatively high-temperature (362 °C), which allowed producing most of the thermal energy needed for solvent regeneration directly in a heat recovery section without the need for a significant fuel excess (about 21% for a 90% carbon capture rate). An onboard CO_2 storage tank was designed for a travelling time of 2–3 days, which could represent a limitation for longer journeys. In their economic evaluation, they calculated a carbon capture cost in the range of 72–151 €/t. Awoyomi et al. [16] expanded the study by analysing a liquefied natural gas (LNG) fuelled ship and introducing exhaust gas recirculation (EGR) to increase the CO_2 concentration at the inlet of the capture section. EGR allowed decreasing the specific heat requirement for solvent regeneration from 10.5 MJ/kg to 7.5 MJ/kg of CO_2 captured, still values well above specific heat requirements for carbon capture at stationary plants. The authors chose NH_3 as a solvent instead of a more conventional monoethanolamine (MEA) based one, and obtained a carbon capture cost of 108–120 €/t of CO_2. Feenstra et al. [17] designed an onboard carbon capture plant for an LNG and diesel engine, using high-temperature flue gas (325-350 °C) to directly provide heat to the carbon capture unit. This allowed to achieve a 90% carbon capture rate without burning any excess fuel. As they obtained carbon capture costs between 93–231 €/t of CO_2 depending on the size of the ship, this study highlighted how economies of scale can play an important role in the economic performance of such systems. Other works on carbon capture onboard ships include that of Long et al. [18], who investigated the decarbonisation of a small diesel ship, that of Ros et al. [19], focused on a 8 MW LNG fuelled crane ship, and the study by Ji et al. [20], who proposed an innovative absorber/stripper design under variation of solvents, packed type, and liquid to gas ratio. Mærsk [21] conducted a study on the application of onboard carbon capture to different classes of ships and fuels, which provided more pessimistic results with respect to Feenstra et al. [17], showing excess energy consumption reaching peaks of 45% for diesel ships and 18% for LNG ones. Another report by OGCI [22] showed similar results in terms of excess energy. This was calculated by using only the available heat from the main propulsion engine, and resulted in capturing only the 8% of the CO_2 in the flue gases. This relatively low figure hints at the lack of waste heat available from the efficient, slow-speed, two-stroke engines. As the target carbon capture rate increases, its energy demand raises, and this is typically supplied through excess fuel burned in the auxiliary engines and fuel fired boilers. In other words, high carbon capture rates require additional (or parasitic) energy, mainly in the form of heat, and if this cannot be provided by the ship itself, it is typically generated by burning more fuel in a boiler, with a significant impact on the environmental and economic performance of the process. This was highlighted in a detailed analysis presented by Einbu et al. [23], which considered variations in engine load and fuel, carbon capture rate, and equipment size.

From an economic perspective, most of the published literature emphasises that capital expenditures constitute the most significant portion of overall costs. This observation can be attributed to their shared emphasis on smaller to medium-sized vessels. Plus, the contribution of some operative costs was often neglected, such as the CO_2

unloading cost and the revenue loss for cargo weight unavailability. The former refers to the fee that the liner must pay to unload at ports the captured CO_2, while the latter arises from the increase in tonnage resulting from the difference in weight between the fuel burned and the CO_2 stored onboard alongside carbon capture operation. These costs depend on the geographic characteristics of the actual journey of the ship. For instance, Negri et al. [24] assumed a fixed distance from geological storage of 200 km; notwithstanding this, the cited work, as well as others discussed above, tested the plant on a medium-sized ship that was designed to operate only for short-distance voyages. Furthermore, even though reporting a container volume reduction related to the installed equipment (which is an aspect not addressed in this study given the significant size of the considered ship), that work did not consider the operative loss due to the increase in mass during navigation alongside the operation of the CO_2 capture plant.

The final aim of this study is to investigate the techno-economic performance of installing and operating a carbon capture plant onboard a large commercial ship. The selected ship is representative of the size of vessels currently travelling from East Asia to North Europe. The novelty of this work is in the combination of these aspects:

- This study focuses on an ultra-large container vessel (190000 t), to appreciate the effect of a substantial ship size (and consequently, with a significant level of CO_2 emissions) on the feasibility and cost of onboard carbon capture.
- The integration of electric heat pumps marks a novelty from the thermal energy recovery-perspective, to provide (part of) the necessary heat to the carbon capture plant. Electric heat pumps are an efficient way to extract thermal energy from a moderate temperature stream and could be a promising solution for heat integration with the low-temperature engine flue gases.
- From an operational standpoint, this study considers a real voyage composed by multiple legs, to provide a holistic understanding of the logistic and economic complexities involved in sizing an onboard carbon capture plant (comprehensive of onboard CO_2 storage vessel). Under the same assumptions (i.e., long-distance, multi-leg trip) the loss of available cargo weight due to onboard carbon capture is also included in the calculations, to assess the economic burdens that shipping companies may need to sustain to operate these systems during a standard journey.

2. Methodology

2.1. Reference ship and flue gas composition

The ship selected for this study is an ultra-large container vessel currently operating between East Asia and North Europe. It has a nominal capacity of 20 568 twenty foot equivalent unit (TEU) and a dead-weight (DWT) of nearly 190 000 t (Table 1). The ship is powered by two MAN engines that are compatible with the vessel requirement. These support dual-fuel operation (i.e., they can run either on LNG or on HFO) and produce nearly 33 MW of nominal power output, each. Operating data such as the engine load, fuel consumption, flue gas flow rate, and temperature were retrieved from MAN CEAS engine calculator for both the LNG and HFO modes (Table 2) (see details in the Supplementary Material). The flue gas composition resulting from combustion was evaluated via the ASPEN Plus software by computing a stoichiometric combustion with imposed total fuel conversion and pre-set flue gas temperature. Fuel flow rates were retrieved from the engine data by assuming a load factor of 80% of the nominal engine power (which is a reasonable value based on current practice for ultra-large container vessels). LNG composition was assumed to be 90%^{mol} of CH_4, 7.5%^{mol} of ethane, and the remaining propane. The composition of HFO was assumed to be 85.1%^{mass} of C, 10.9%^{mass} of H, and the remaining 4%^{mass} being sulphur. As a result, the two LNG engines produce a flue gas with a flow rate of 114.2 kg/s, available at a temperature of 206 °C.

Table 1
Reference ship and propulsion data. TEU is the standard size of a container. DWT is the difference between the displacement and the mass of empty vessel (light-weight) at any given draught, in other terms the maximum weight a ship can carry.

Ship characteristics	
DWT	190300 t
TEU	20 568
Construction year	2017
Engine nominal power output	65940 kW
Engine type	7G80ME-C10.5-GI-HPSCR Gas Opt.
Number of engines	2
Engine fuel	Dual fuel: LNG or HFO.

Table 2
Summary of flue gas characteristics depending on LNG or HFO operation mode. Impurities are not reported, nor included in the simulations (e.g., Ar, S).

Flue gas		Unit	Operation mode	
			LNG	HFO
Temperature		[°C]	206	214
Mass flow rate		[kg/s]	114.2	122.4
Molar flow rate		[kmol/s]	3.99	4.21
Molar fractions	H_2O	[%^{mol}]	5.84	3.05
	CO_2	[%^{mol}]	3.06	4.00
	O_2	[%^{mol}]	14.40	15.10
	N_2	[%^{mol}]	75.70	76.80
	Traces	[%^{mol}]	1.00	1.05

This gas contains 3.06%^{mol} CO_2 on a wet basis (3.25%^{mol} CO_2 on a dry basis). Differently, the HFO propulsion generates a flue gas with a flow rate of 122.4 kg/s. This gas has a higher CO_2 content, equal to 4.00%^{mol} CO_2 on a wet basis (4.12%^{mol} CO_2 on a dry basis), and a temperature of 214 °C. This difference in CO_2 concentration is primarily attributed to the larger carbon-to-hydrogen (C/H) ratio in HFO compared to LNG. It is also important to note that, for the same power output, the flue gas flow rate is higher for HFO due to its lower calorific value compared to LNG. As a result, by considering 4 roundtrips per year (i.e., more than 8000 h/year of operation), the ship produces about 150 kt/year of CO_2 if fuelled with LNG, and about 210 kt/year if fed with HFO. As for SOx and NOx pollutants, we assume that the ship is already equipped with relevant abatement systems; hence, these are excluded from the calculations.

The objective is to abate the CO_2 emissions deriving from the fuel combustion in the main propulsion engines of the ship described above. As such, the proposed plant scheme is composed by: (*i*) a carbon capture unit, which separates the CO_2 from the flue gases; (*ii*) a low-temperature purification and liquefaction unit, to increase the CO_2 concentration for a cost-effective handling and operation; and (*iii*) a storage tank, to keep the CO_2 in liquid state during the voyage.

2.2. Plant design configurations

Fig. 1 shows the simplified schemes of the CO_2 capture configurations analysed in this study. The base configuration (Fig. 1(a)) is characterised by heat integration with the hot flue gases (Case Flue Gas — Case FG). The hot flue gases deriving from the ship engines provide heat to cover the thermal duty of the carbon capture system. As the results will demonstrate, the heat that can be extracted in this case is in a limited quantity compared with the thermal duty of the carbon capture plant; hence, Case FG can achieve only a partial CO_2 separation. To overcome this and obtain higher values of carbon capture rate, one option (Fig. 1(b)) is to burn additional fuel (to that one already deployed in the ship engines) in a fuel-fired steam boiler (Case Fuel Boiler — Case FB). As this option produces a significant amount of parasite CO_2 emissions due to the fossil fuel combustion, an alternative design (Fig. 1(c)) investigates the integration of electric heat pumps (Case Heat Pump — Case HP) for the exploitation of residual and low-temperature heat. The plants were simulated in Aspen Plus

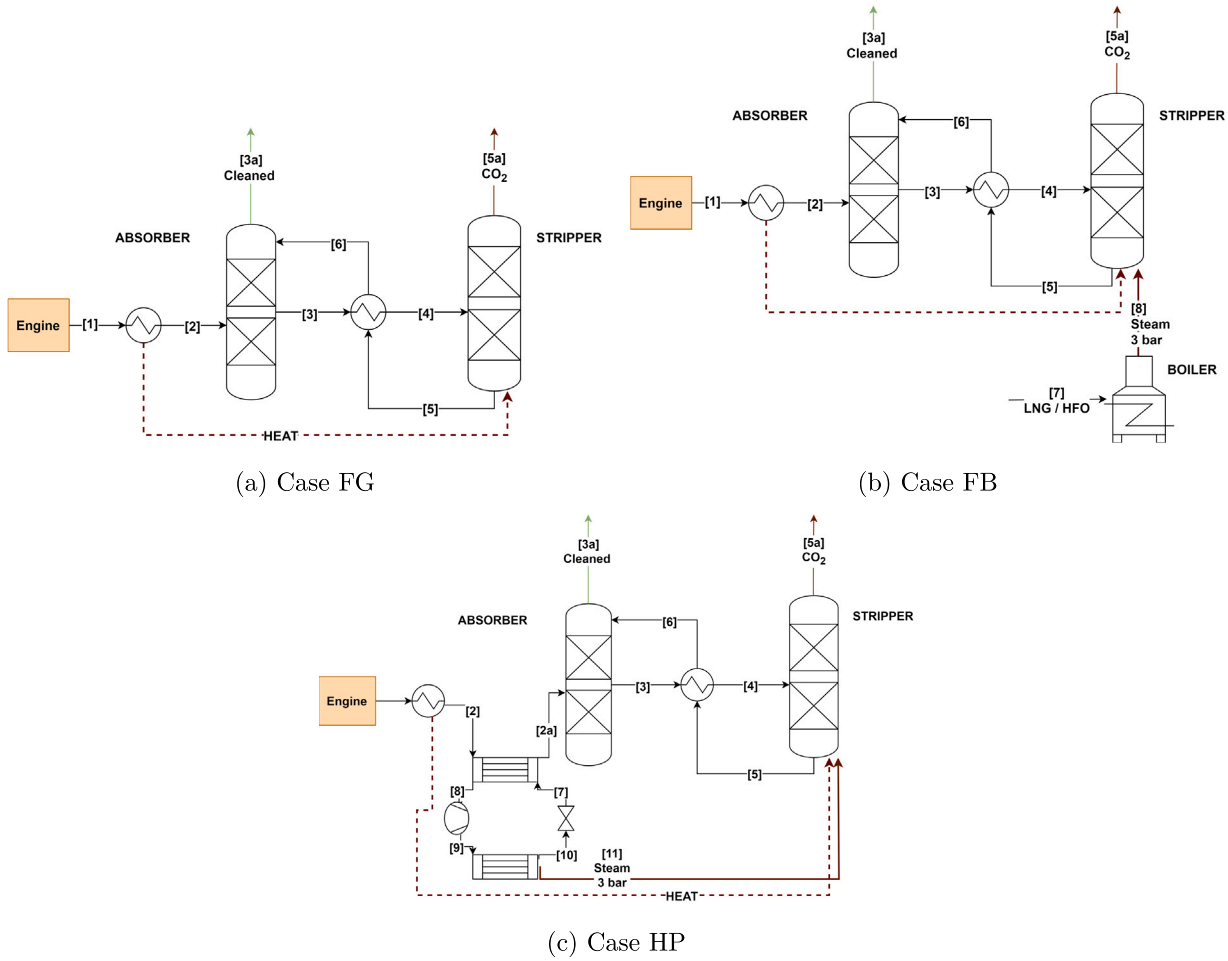

(a) Case FG

(b) Case FB

(c) Case HP

Fig. 1. Simplified flowsheets of plant configurations: (a) base case with heat integration on hot flue gases (Case FG); (b) fuel boiler integration (Case FB); (c) electric heat pump integration (Case HP).

software by using the Peng–Robinson equations of state. The detailed process schemes will be presented in the next sections.

2.3. Carbon capture unit

In the base configuration (Case FG) the hot flue gas is deployed to provide heat to the reboiler to cover the thermal energy required for the MEA solvent regeneration in the stripper column (Streams #1-#2, Fig. 2). The minimum temperature difference between hot and cold streams is set at 30 °C. The flue gas is then cooled down with seawater (#13), assumed to be available at 10 °C, in order to partially condense H_2O, increase the CO_2 concentration, and reduce the temperature at the inlet of the absorber. This is done to increase the absorption capacity of MEA, considering the thermodynamics of the exothermic CO_2 absorption system that could cause reversible reactions when the temperature is too high [25]. Furthermore, the increase in temperature would lead to a decrease in the physical solubility of CO_2 in the solvent [25]. The cooled exhaust gas is then fed to the bottom of the absorber (#3), where it is contacted in countercurrent with an aqueous MEA solution (#10). The MEA solution is able to chemically absorb the CO_2, allowing the cleaned flue gas to exit the column. The off-gases (#11) of the absorber are then cooled down with seawater in order to recover the MEA solvent, which is then recirculated back to the column. After this step, the cleaned-up gas, containing only a minor fraction of solvent, is emitted to the atmosphere (#12). The CO_2-rich stream exiting from the bottom of the absorber is heated up with the regenerated solvent coming from the stripper (#4-#5). Then, the heated stream (#5) is charged at the top of the column. In the stripper column, the inverse process of the absorber occurs in an endothermic reaction, and the CO_2 exits as a gas from the top (#6) while the regenerated solvent solution is recovered from the bottom (#8) and is recirculated back to the absorber. The CO_2-rich stream is then cooled down with seawater (#6-#7) to recover the solvent and further increase the concentration of CO_2. As for the columns, in agreement with Feenstra et al. [17] and Agbonghae et al. [26], a structured packing is chosen in this work.

In Case FB, alongside heat integration with the hot flue gases as in Case FG, additional fuel to that employed for the ship engines is burned in a steam boiler to generate more low-pressure steam to the stripper reboiler. This is done to increase the CO_2 capture performance of the onboard carbon capture system, at the cost of producing additional CO_2 emissions due to the direct combustion of a fossil fuel in the boiler.

In the case of electric heat pump integration (Case HP), this is implemented on the hot flue gas stream available at 150 °C (Stream #2, Fig. 3). A single-stage heat-pump layout is chosen due to the temperature lift being lower than 60 °C and being the compression ratio limited to 4. The refrigerant employed is R1233ZD; the choice was based on the set of temperatures involved in order to maximise the coefficient of performance (COP) [27], being this defined as the ratio between the provided heat and the consumed electric power. The flue gas stream is cooled down to 85 °C (Stream #2a) by evaporating the refrigerant, which in turn is compressed from 6 bar to 24 bar (#17-#18), with the temperature increasing from 139 °C to 196 °C. The heated refrigerant is then condensed to produce low-pressure steam at 3 bar (#18-#19). This steam provides the thermal energy to the

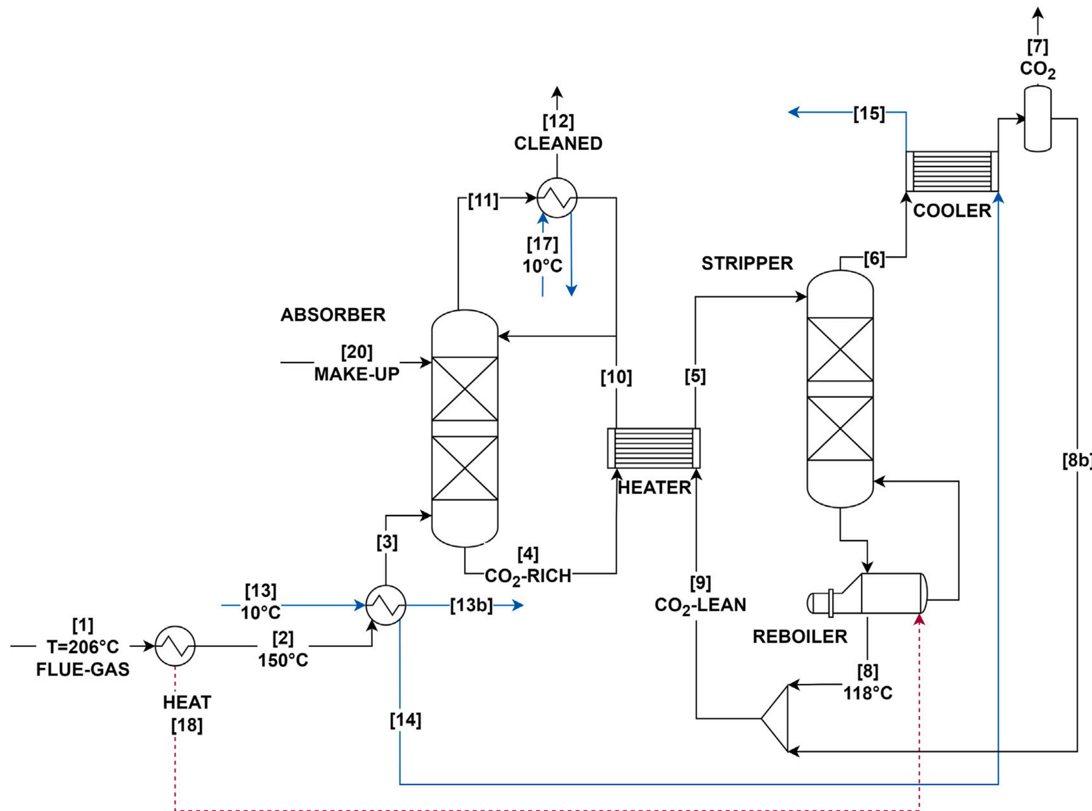

Fig. 2. Case FG: carbon capture plant flowsheet. The seawater for cooling is represented in blue colour, while the dashed red line represents the heat integration between the hot flue gas and the stripper reboiler. An additional heat stream to the stripper reboiler would be present in Case FB (not represented here). The detailed streams properties and compositions are reported in the Supplementary Material.

reboiler of the carbon capture unit, alongside that extracted from the hot flue gases through direct heat integration.

To compare the performance of Case FG, Case FB, and Case HP, the excess fuel flow rate $\dot{m}_{fuel}$ [kg/s] that is needed to sustain the additional (or parasitic) consumptions for carbon capture, purification, and liquefaction is computed as:

$$\dot{m}_{fuel} = \frac{\dot{Q}_{reb} - \dot{Q}_{available}}{\dot{m}_{fuel,boiler} \cdot LHV_{fuel,boiler} \cdot \eta_{boiler}} + \frac{\dot{W}_{comp}}{\dot{m}_{fuel,engine} \cdot LHV_{fuel,engine} \cdot \eta_{engine}} \quad (1)$$

where the first term refers to the additional fuel consumption to generate heat for solvent regeneration, given by the difference between that available from hot flue gas integration $\dot{Q}_{available}$ [MW_{th}] and the reboiler duty $\dot{Q}_{reb}$ [MW_{th}], in the case this thermal power is provided via a conventional steam boiler with efficiency η_{boiler} of 95%. The second term reflects the fuel consumption to support the electric power generation for the compressor(s) (for the compression and purification unit, but also for the electric heat pump in Case HP) $\dot{W}_{comp}$ [MW_{el}], depending on the efficiency of the ship engine η_{engine} [%], which corresponds to 27.78 MJ_{el}/kg (LNG) and 22.19 MJ_{el}/kg (HFO). These efficiencies are retrieved from the engine datasheet at the operating load factor, as well as the lower heating values (LHV) of fuels, equal to 42.7 MJ/kg for HFO and 50 MJ/kg for LNG (see Supplementary Material).

2.4. Purification, liquefaction, and storage tank

After CO_2 capture, a purification process is needed to separate the non-condensible gases and the remaining H_2O. Then, the purified CO_2 must be liquefied for storage, with the additional requirement of H_2O removal to prevent freezing. The thermodynamic model for these unit is based on the Peng–Robinson equations of state as in Deng et al. [28]. Depending on the ship fuel, the gaseous stream is treated in different ways. In the case of LNG fuelled ship, it is compressed to 15 bar with a 2-stage compressor with an isentropic efficiency of 85% (Streams #1-#5, Fig. 4(a)), with a resulting CO_2 concentration of 99.3%^{mol}. This level of purity is considered suitable for geological storage [29]. The purified CO_2 is then liquefied by using the evaporating LNG as a cooling medium (#5-#6), similarly to the scheme proposed in Awoyomi et al. [16] and Feenstra et al. [17]. Differently, in the case of the HFO fuelled ship, the stream is compressed to 15 bar under the same assumptions of the LNG case (Streams #1-#5, Fig. 4(b)), but after purification the cooling requirement is met by implementing a NH_3-based refrigeration cycle (#6-#11). The liquefied CO_2 is subsequently laminated and stored in tanks at low pressure (9 bar, -45 °C), in line with the findings of Roussanaly et al. [30]. These thermodynamic conditions are chosen to avoid entering a bi-phase region after lamination, while keeping a low-pressure design to minimise chain costs [30].

2.5. Economic model

The total annual cost TAC [M€/y] is computed by taking into account the annualised capital expenditures ($CAPEX_y$) [M€/y], the fixed operational expenditure ($fOPEX$) [M€/y], and the variable ones ($VOPEX$) [M€/y]:

$$TAC = CAPEX_y + fOPEX + vOPEX \quad (2)$$

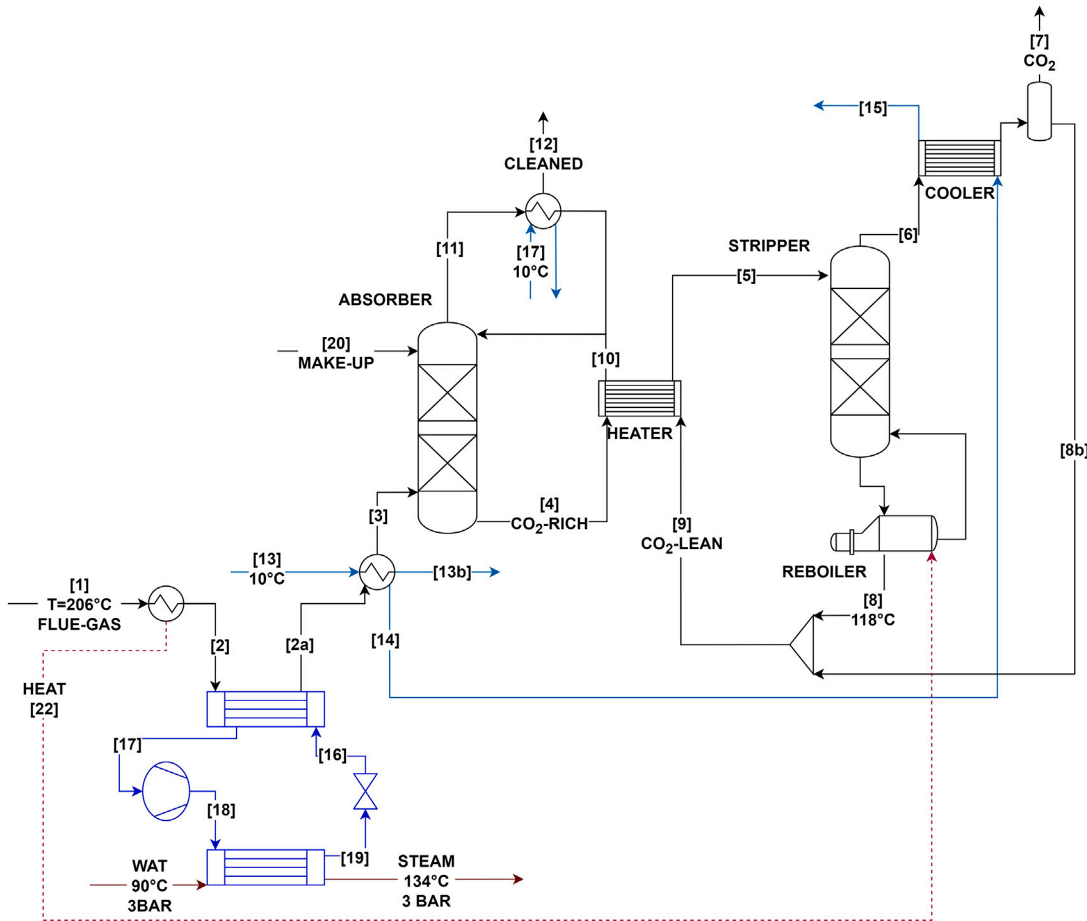

Fig. 3. Case HP: carbon capture plant flowsheet. The steam cycles are closed (not shown for graphic reasons). The detailed streams properties and compositions are reported in the Supplementary Material.

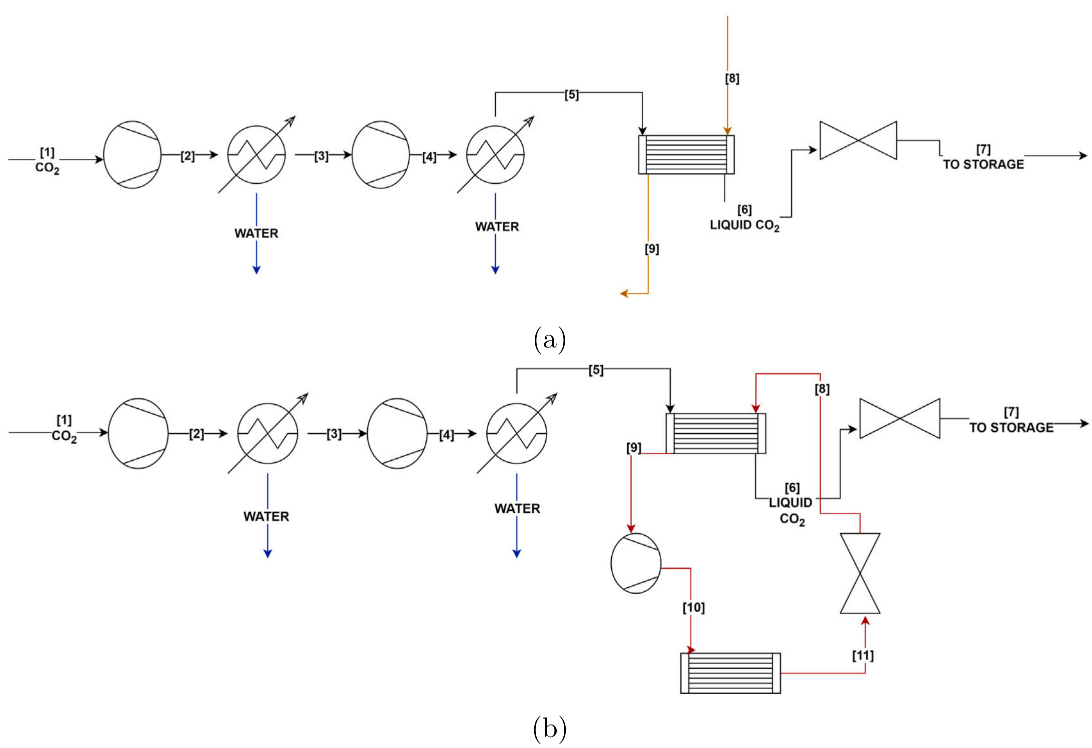

Fig. 4. Purification and liquefaction section flowsheets for: (a) LNG fuelled ship; and (b) HFO fuelled ship.

Table 3
Equipment purchase price coefficients referred to Eq. (3) from Towler and Sinnott [31]. Results are updated through CEPCI ($\$^{2019}/\$^{2006}$ equal to 607.5/499.6), and converted through €/$ (1.06).

Unit	S [S]	a [$]	b [$/S]	n [–]	f [–]
Absorber	Shell mass [kg]	−10000	600	0.6	4.0
	Packing [m^3]	0	3200	1.0	4.0
Stripper	Shell mass [kg]	−10000	600	0.6	4.0
	Packing [m^3]	0	3200	1.0	4.0
Compressor	Shaft power [MW]	8400	3100	0.6	2.5
Reboiler	Excha. Area [m^2]	14 000	83	1.0	3.5
Condenser	Excha. Area [m^2]	10 000	88	1.0	3.5
Storage tank	Volume [m^3]	0	643	1.0	1.0
Flash tank	Shell mass [kg]	−10000	600	0.6	4.0

The annualised capital expenditures $CAPEX_y$ of Eq. (2) depend on the capital expenditures $CAPEX$ [M€]. For each process unit,[1] the equipment purchase price C [€] is evaluated according to Towler and Sinnott [31]:

$$C = a + b \cdot S^n \tag{3}$$

where a [€] and b [€/relevant unit] are equipment-dependent parameters, S [relevant unit] is the relevant equipment size measure and n [–] is a scaling exponential coefficient (Table 3). To evaluate the inside battery limits plant cost $ISBL$ [€] cost, an installation factor f is applied on each unit [33]:

$$ISBL = C \cdot f \tag{4}$$

The fixed capital investments FCI [€] is calculated by considering a 14% increment to $ISBL$ due to indirect construction costs [34]:

$$FCI = ISBL \cdot (1 + 0.14) \tag{5}$$

Finally, the $CAPEX$ accounts also for start-up costs, contingencies, capital fees, and working capital [34]:

$$CAPEX = FCI/0.8 \tag{6}$$

The annualised $CAPEX_y$ is evaluated considering a 25 years lifetime t and an interest rate i of 8%:

$$CAPEX_y = CAPEX \cdot \frac{i \cdot (i+1)^t}{(i+1)^t - 1} \tag{7}$$

Fixed operating costs $fOPEX$ of Eq. (2) refer to long-term service arrangement costs, overhead costs, maintenance and labour cost, and are assumed equal to 3% of $CAPEX_y$ [34]:

$$fOPEX = CAPEX_y \cdot 0.03 \tag{8}$$

Variable operative expenditures $vOPEX$ of Eq. (2) depend on the yearly cost for fuel (C_{fuel} [M€/y]), for MEA solvent (C_{MEA} [M€/y]), for CO_2 unloading (associated to transport and geological storage costs downstream unloading) ($C_{T\&S}$ [M€/y]), and for the loss of revenues due to reduced transport capacity (C_{cargo} [M€/y]):

$$vOPEX = C_{fuel} + C_{MEA} + C_{T\&S} + C_{cargo} \tag{9}$$

where the cost of fuel and that of MEA depend on the yearly additional fuel needed to operate capture ($\hat{m}_{fuel}$ [t/y]) derived from Eq. (1) and on the yearly fresh solvent requirements ($\hat{m}_{MEA}$ [t/y]), respectively, and on their unitary costs (c_{fuel} [535 €/t of LNG, 448 €/t of HFO] [35] and c_{MEA} [1350 €/t of MEA]) [16]:

$$C_{fuel} = \hat{m}_{fuel} \cdot c_{fuel} \tag{10}$$

[1] Differently, in the case of the fuel boiler of Case FB, its equipment purchase price S is derived from NETL [32]. As this cost is marginal compared to other units and given its final purpose (i.e., generating low-pressure steam), the results will include its contribution in the cost of heat exchangers.

$$C_{MEA} = \hat{m}_{MEA} \cdot c_{MEA} \tag{11}$$

As for $C_{T\&S}$ of Eq. (9), this depends on the specific geographic context. In order to give general validity to the study, it was assumed that CO_2 transport from the unloading port to geological sequestration can vary between 4.6 €/t (100 km CO_2 transport via pipeline, for unloading scenarios assuming integration with onshore CO_2 infrastructures) and 14.8 €/t (1500 km CO_2 transport via ship), for other unloading scenarios [36]. A subsequent section on the analysed case studies will clarify these assumptions. As for sequestration costs, this study assumes 9.3 €/t [37], which is in line with d'Amore et al. [38]. Note that this study does not account for the contribution of fresh H_2O make-up to variable costs, as it is assumed that its cost would represent a marginal fraction of the overall expenditure for the system.

The value of C_{cargo} of Eq. (9) depends on the variation of the cargo load profile across the journey. This study assumes that the total weight of the baseline ship (DWT_k [t]) is constant across the entire journey and for all the legs k, and that the ship must refuel once the fuel tank is empty by 50%. When carbon capture is implemented and operated onboard the ship, this produces a loss of available cargo weight due to the difference in mass between the CO_2 captured and stored onboard and the fuel burned during the leg. For instance, considering the LNG fuelled ship, for every kg of fuel burned, nearly 2.83 kg of CO_2 are produced. This effect is even more important in the case of the HFO fuelled ship, in which 3.11 kg of CO_2 are generated for every kg of fuel burned. Accordingly, for every leg k:

$$DWT_k = m_{fuel,k} + m_{cargo,k} + m_{CO_2,k} = const \tag{12}$$

This has the effect of reducing the cargo capacity of the ship alongside onboard CO_2 storage, with a consequent loss of revenues (i.e., C_{cargo}) from the transportation of containers, which can be expressed as:

$$C_{cargo} = fr \cdot \sum_k (\Delta m_{cargo,k} \cdot \frac{d_{tot} - d_k}{d_{tot}}) \tag{13}$$

where fr is the freight rate per forty foot equivalent unit containers (FEU) associated with the voyage, d_{tot} [days] is the entire duration of the voyage expressed in days, and d_k [days] is the time required for the leg k. Regarding the freight rates fr, they were retrieved from the Drewry World Container Index [39], which measures the bi-weekly ocean freight rate movements of 40-foot containers in seven major maritime lanes. In particular, as detailed in the subsequent section, the selected ship travels between Shanghai and Rotterdam and for this route the freight rate is equal to 1128 €/FEU (Shanghai-Rotterdam) and 528 €/FEU (Rotterdam-Shanghai).

3. Case study

As a reference trip, it is assumed that the ship travels between Shanghai and Rotterdam, major container hubs. The capacity profiles of the baseline ship (i.e., without CO_2 capture) are reported in Fig. 5 for the LNG and HFO fuelled options. The LNG fuelled ship needs to refuel more often (at legs 8, 15, and 19) than the HFO one (one stop at leg 15). Based on this journey, three possible CO_2 unloading scenarios were defined, depending on the hypothetical availability of an onshore CO_2 infrastructure downstream the unloading from the ship:

- Scenario 1 (S1). The ship can unload the CO_2 at every port in which it stops. This is an optimistic scenario which assumes a mature CO_2 network development.
- Scenario 2 (S2). The ship can unload the CO_2 one at every two ports. This scenario is built to evaluate the impact of unloading availability on the flexibility of the ship (e.g., loading fuel and cargo variations).

Table 4
Port calls and leg duration [days].

Port	Leg	Duration [days]	Port	Leg	Duration [days]
Shanghai	0	0	Bremerhaven	11	3
Dalian	1	1	Gothenburg	12	3
Xingang	2	1	Aarhus	13	1
Busan	3	2	Bremerhaven	14	2
Ulsan	4	1	Wilhelmshaven	15	1
Ningbo	5	2	Port Tangier	16	5
Shanghai	6	1	Suez Canal	17	5
Tanjung Pelepas	7	5	Suez Canal	18	1
Suez Canal	8	11	Singapore	19	13
Suez Canal	9	1	Shanghai	20	5
Rotterdam	10	8			

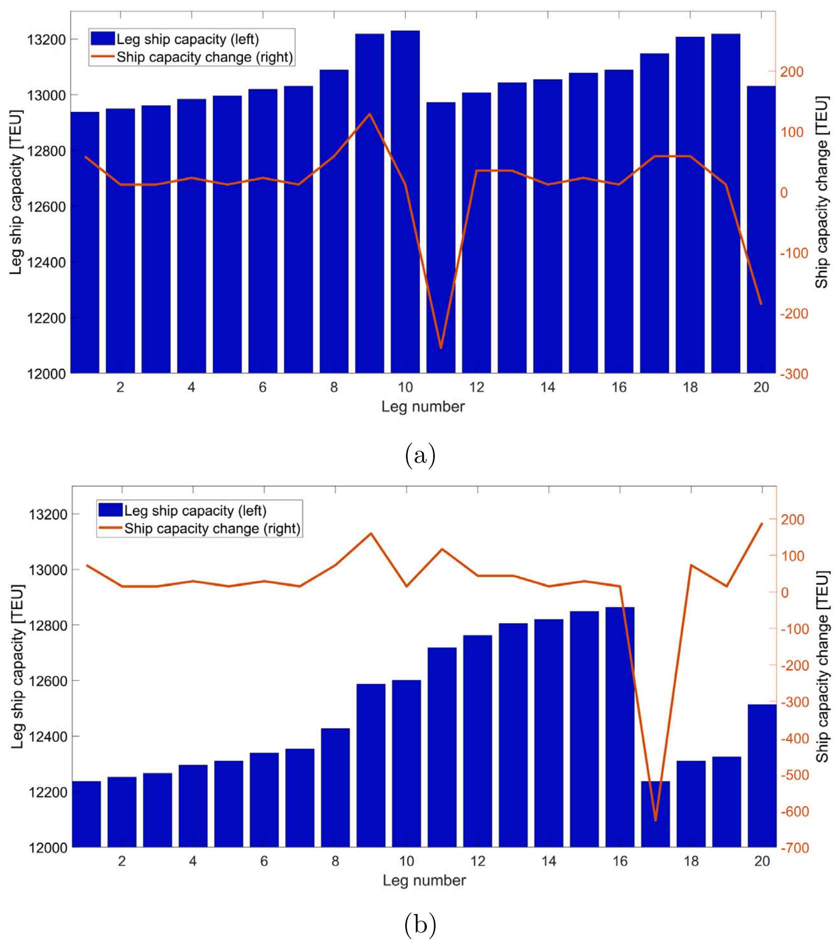

Fig. 5. Baseline ship (i.e., without CO_2 capture) capacity profiles for: (a) LNG fuelled ship; and (b) HFO fuelled ship.

- Scenario 3 (S3). This scenario tests the impact of a modest and jeopardised future development of onshore CO_2 networks. This scenario assumes that the ship cannot unload the CO_2 in Singapore, Suez, or Tangier ports, while the remaining ones (Table 4) are equipped for CO_2 handling downstream the ship.

4. Results

4.1. Technical analysis

The technical results are summarised in Table 5. The concept behind Case FG is to design a carbon capture plant with limited (or partial) separation performance, so that its thermal requirement can be completely fulfilled via heat integration with the hot exhaust gas stream from the ship engines. The carbon capture rate is limited to 36.3% (LNG ship) and to 32.6% (HFO ship), as a result of a specific reboiler duty of 3.43 MJ/kg and 3.31 MJ/kg, respectively. Due to the different flue gas flow rate and composition between LNG and HFO operation, these plants are designed to capture 1.97 kg/s (LNG ship) and 2.47 kg/s (HFO ship) of CO_2, and require 0.4 MW_{el} (LNG ship) and 1.0 MW_{el} (HFO ship) to operate the purification and liquefaction plant downstream CO_2 separation, which are provided via the ship engines. As the additional fuel combustion to operate the purification and liquefaction unit is modest (+0.5% and +1.2% for LNG and HFO ships, respectively), this produces a limited amount of parasitic CO_2 emissions. As such, the performance in terms of capture and avoidance rate, defined as the relative net CO_2 savings with respect to the reference ship without capture, is quite similar, which is not the case of other investigated options.

As for Case FB for the LNG fuelled engine, the results show that to achieve a 90% CO_2 separation rate at the carbon capture unit, 17.1

Table 5
Technical results: Case studies, plant design, and performance indicators. Case 'ship' refers to the baseline ship without onboard carbon capture.

Case study		ship	FG	FB	HP	ship	FG	FB	HP
Ship fuel		LNG				HFO			
Flue gas heat		no	yes	yes	yes	no	yes	yes	yes
Steam boiler		no	no	yes	no	no	no	yes	no
Heat pump		no	no	no	yes	no	no	no	yes
Carbon capture unit									
Absorber diameter	[m]	–	5.0	5.5	5.5	–	5.5	5.5	5.5
Stripper diameter	[m]	–	1.8	2.5	2.5	–	2.0	3.0	2.5
Heat pump compr.	[MW_{el}]	–	0.0	0.0	2.5	–	0.0	0.0	2.3
Flue gas heat	[MW_{th}]	–	6.8	6.8	6.8	–	8.2	8.2	8.2
Reboiler duty	[MW_{th}]	–	6.8	17.1	17.6	–	8.2	23.6	17.9
Spec. reboiler duty	[MJ/kg]	–	3.43	3.54	3.62	–	3.31	3.57	3.38
Purification and liquefaction unit									
CO_2 purity	[%^{mol}]	–	99.8%	99.3%	99.3%	–	99.3%	99.3%	99.3%
Other compressor(s)	[MW_{el}]	–	0.4	1.2	1.2	–	1.0	2.7	2.1
Purification pressure	[bara]	–	15	15	15	–	15	15	15
Storage pressure	[bara]	–	9	9	9	–	9	9	9
Onboard storage tank									
Volume (S1)	[m^3]	–	1930	4825	4825	–	2437	6647	5317
Volume (S2)	[m^3]	–	2078	5196	5196	–	2624	7158	5726
Volume (S3)	[m^3]	–	4304	10 763	10 763	–	5435	14 827	11 861
Performance indicators									
CO_2 emitted	[kg/s]	5.38	3.46	1.37	0.97	7.41	5.10	2.62	2.82
CO_2 captured	[kg/s]	0.00	1.97	4.84	4.84	0.00	2.47	6.67	5.31
CO_2 avoided	[kg/s]	0.00	1.92	4.01	4.41	0.00	2.31	4.79	4.59
Fuel excess (capt.)	[%]	–	0.0%	11.0%	4.7%	–	0.0%	17.0%	4.4%
Fuel excess (purif. liq.)	[%]	–	0.5%	2.1%	2.1%	–	1.2%	5.0%	4.2%
CO_2 capt. rate (capt. unit)	[%]	0.0%	36.6%	89.9%	89.9%	0.0%	33.3%	90.0%	71.7%
CO_2 capt. rate (total)	[%]	0.0%	36.3%	77.9%	83.3%	0.0%	32.6%	71.8%	65.3%
CO_2 avoidance rate	[%]	0.0%	35.4%	64.5%	75.9%	0.0%	30.5%	51.6%	56.4%

MW_{th} are needed to cover the thermal duty of the reboiler. However, the heat integration with the engines hot flue gases can only provide 6.8 MW_{th}, while the remaining is covered by burning LNG in a steam boiler, which brings the total (or net) carbon capture rate to 77.9%, corresponding to a CO_2 avoidance rate of 64.5%, due to the increased fuel consumption associated (mainly) to heating.[2] The results for the HFO option for Case FB are similar. The main difference is the higher CO_2 captured flow rate, equal to 6.67 kg/s, determining an excess HFO consumption of +0.4 kg/s (i.e., +17%) with respect to the baseline ship without capture. This produces a total (or net) CO_2 capture rate of 71.8% and a CO_2 avoidance rate of 51.6%. The reboiler duty is 23.6 MW_{th}, being only 8.2 MW_{th} provided by heat integration with the ship exhaust gas. In Case FB, for the HFO-fed ship the specific reboiler duty is 3.57 MJ/kg; hence, it is comparable with that obtained in the case utilising LNG (3.54 MJ/kg). This result suggests that the higher CO_2 concentration in the flue gas of the HFO case is not sufficient to positively impact in a substantial way the efficiency of the carbon capture process, because it is negatively compensated by the higher flow rate of solvent required to achieve a significant carbon capture rate.

The electric heat pump integration (Case HP) produces a decrease in the inlet temperature to the absorber compared to Case FB. As for Case HP for the LNG-fed ship, this is characterised by a slightly higher reboiler duty (17.6 MW_{th}), and consequently by an increase in the specific reboiler duty, with respect to its corresponding Case FB. However, the heat pump effectively supplies (part of) the necessary thermal energy with an electricity demand of 2.5 MW_{el} (corresponding to a COP of 4.3). This translates into a slight increase in LNG consumption of +0.09 kg/s (i.e., +4.7%), with respect to the baseline ship without capture. Notably, this value is much lower (−56.9%) than that obtained in the corresponding Case FB, which reflects in a better performance of Case HP in terms of CO_2 avoidance. In fact, the resulting total carbon capture rate is 83.3%, for a CO_2 avoidance of 75.9% with respect to the baseline LNG ship without capture. In the HFO option (Case HP), due to the higher flue gas flow rate compared with LNG case, the electric heat pump is unable to provide sufficient thermal energy to achieve a 90% separation at the carbon capture unit. As a result, the 71.7% of the CO_2 entering this unit is effectively separated, which corresponds to a total carbon capture rate of 65.3%, or to a CO_2 avoidance rate of 56.4% with respect to the benchmark HFO ship without capture. This result highlights that the fuel of the ship has a strong influence on the applicability of the heat pumps and, more in general, on the technical impact of the carbon capture plant on ship operations, though the integration of a heat pump system could play a pivotal role in reducing parasitic fuel consumptions also when considering HFO-fed ships.

In general, from the comparison between Case FB and Case HP, it emerges that the specific reboiler duty is not the primary parameter for evaluating the separation performance of the capture process. If it were the case, the plant would be designed to maximise the excess steam production in order to preheat the feed to the stripper column and reduce the reboiler duty. However, this approach leads to an increase in excess fuel consumption (i.e., the additional fuel needed to meet the thermal energy demand), that would result in higher operating costs and in increased parasitic CO_2 production. As such, if the goal is to achieve a significant carbon capture rate while minimising the cost of capture, the key parameter to focus on for onboard applications is the excess fuel, which should be minimised. As the minimisation of this parameter is related to the low-pressure steam production route, using a heat pump can allow the plant to recover a greater amount of heat with a lower amount of additional fuel thus, lowering the overall external energy supply.

As for the capture unit design (Table 5), the stripping column shows significant differences among the analysed cases. In fact, its diameter

[2] Our process implies not to capture the parasitic CO_2 generated for fulfilling the capture system energy requirements, which clearly reflects in the large distance between capture and avoidance performance in most of the analysed cases. For Case FB (LNG ship) it was verified that capturing also the parasitic CO_2 would determine an increase in fuel consumption of more than +16% with respect to the baseline LNG ship without capture.

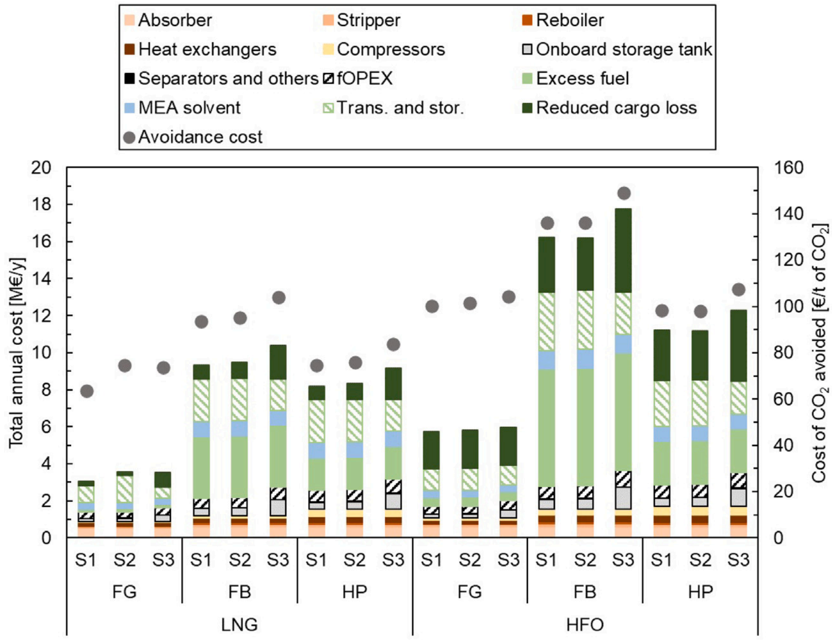

(a)

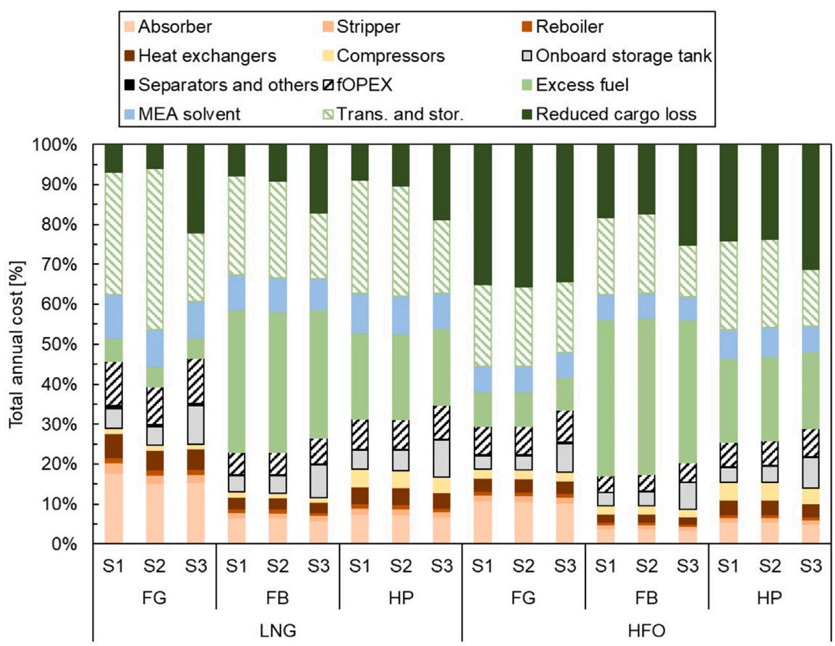

(b)

Fig. 6. Economic results: (a) total annual cost breakdown [M€/y] and cost of CO_2 avoided [€/t of CO_2] (represented in grey circles), and (b) percentage total annual cost breakdown [%].

ranges from 1.8 m to 2.5 m in the LNG fuelled cases, while it increases up to 3 metres for the HFO ones. This could challenge the dual fuel engine utilisation mode and limit the operability of the capture plant. Differently, the absorber does not pose any particular challenges to its onboard installation, having a diameter nearly constant among the analysed cases (between 5 and 5.5 m) and a height around 20 m, which is compatible with installation onboard an ultra-large container vessel. With reference to the purification and liquefaction unit, all the plants are able to achieve a CO_2 purity above 99%^{mol}, with the main difference being in the energy demand. In particular, in the LNG cases this purity can be achieved without the need for the NH_3 cycle, with beneficial effects in terms of energy consumptions (−30%) with respect to HFO fuelled options. The electricity required for CO_2 purification and liquefaction is provided by the engines. For instance, in Case FB this results in an auxiliary fuel consumption for purification and liquefaction of 0.04 kg/s (Case FB for LNG ship) and 0.12 kg/s (Case FB for HFO ship), which corresponds to the 19% and 30%, respectively, of the total excess fuel required for the overall CO_2 capture, purification, and liquefaction process.

Downstream capture, purification, and liquefaction units, the CO_2 is stored in tanks (9 bar, -45 °C) onboard the ship (Table 5). In the first unloading scenario (S1), onboard CO_2 storage requirements depend mostly on the type of fuel and on the length of legs, as in this case it is (optimistically) assumed that the CO_2 can be unloaded from the ship at every port. As a result, S1 exhibits the lowest volumes for storage among the analysed option, up to 4825 m^3 for LNG and to 6647 m^3 for HFO ships. Differently, in the third scenario (S3), volume requirements are three times larger than those obtained in S1, while in S2 the increase in storage requirements is between +20% and +30% with respect to the results of S1. Furthermore, it is possible to observe that the HFO fuelled ship needs larger storage tanks than the LNG one, due to the higher CO_2 flow rate of the former. If on the one hand the size of these tanks does not represent an issue in terms of loss of cargo volume for an ultra-large container vessel, on the flip side the increase in weight throughout the journey alongside CO_2 capture operation represents a challenge and it reflects into a loss of revenues, as it will be highlighted in the economic outcomes.

4.2. Economic analysis

The economic results are reported in Table 6 and summarised in Fig. 6. As for CAPEX, LNG operation helps decreasing it (11.3–25.8 M€) with respect to HFO navigation (13.7–28.6 M€), due to the lower flue gas flow rate to be treated by the onboard capture plant. Case FG is the least capital intensive due to its limited carbon abatement potential (11.3–13.3 M€ for LNG ship, 13.7–16.3 M€ for HFO one). Differently, Case FB involves a higher carbon capture rate and consequently it exhibits values of CAPEX up to 22.3 M€ for the LNG-fed ship and up to 29.3 M€ for HFO operation. Case HP is always slightly more expensive than Case FB, mainly due to the higher investment cost for the heat pump compressors. Depending on the chosen unloading scenario, Case HP involves a total CAPEX of up to 25.8 M€ (LNG ship) and up to 28.6 M€ (HFO ship). Independently from the plant configuration, the absorber is a significant contributor to the total CAPEX (23%–52%), followed by the onboard storage tanks (15%–43%, being this significant span depending on the choice in the unloading scenario), heat exchangers (12%–18%), and, in Case HP, compressors (up to 23%).

Operative expenditures represent the greatest share of the total annual cost in all the analysed plants (Fig. 6). Case FG is (almost) self-sufficient in terms of energy balance, as such the expenditure for excess fuel is relatively modest and equal to 0.2 M€/y (LNG ship) and 0.5 M€/y (HFO ship). Other significant variable costs include that for MEA solvent (up to 0.8 M€/y for LNG ship, up to 1.0 M€/y for HFO ship), for CO_2 transport and storage (0.6–1.4 M€/y for LNG ship, 1.1–1.2 M€/y for HFO ship), and reduced cargo loss (0.2–0.8 M€/y for LNG ship, around 2 M€/y for HFO ship). As for Case FB and Case HP, these involve variable expenditures for solvent, CO_2 transport and storage, and reduced cargo loss that are proportionally higher than those of Case FG due to the larger flow rate of CO_2 captured in these cases, while the main effect on yearly costs is driven by the significant excess fuel (needed mainly to compensate for the lack of heat for solvent regeneration as highlighted in the technical results). In fact, Case FB exhibits a fuel annual cost of 3.3 M€/y (LNG ship) and 6.4 M€/y (HFO ship), while Case HP can allow for some savings in terms of excess fuel and results in an associated expenditure of 1.8 M€/y (LNG ship) and 2.4 M€/y (HFO ship).

The total annual cost highlights the macroscopic differences in terms of economic outcome among the analysed plants and unloading scenarios. HFO-fed ships involve higher total annual costs in all the analysed cases. On average among S1-S3, Case FG, Case FB, and Case HP are 74%, 72%, and 35% more expensive than their corresponding LNG-based alternatives, mainly due to the higher flue gas flow rate of HFO ship operation. At the same time, the choice of unloading the CO_2 only at some ports that are relevant for an unloading infrastructure (i.e., S3) determines an increase in total annual cost between +4% (Case FG, HFO ship) and +16% (Case FG, LNG ship) with respect to S1, which is mainly driven by the reduced cargo transportation potential. Case HP allows for some savings with respect to Case HP in the LNG configuration (−12%) thanks to its lower fuel costs. In the HFO-fed ship, Case HP seems to determine a significant decrease in total annual cost with respect to Case FB (−31%), but this outcome is mainly related to the different carbon capture rates between these configurations (Table 5). More in general, as the analysed plants are characterised by different level of CO_2 capture and different energy sources for CO_2 separation, compression, and purification, a more realistic assessment of their economic performance can be provided by comparing their cost of CO_2 avoided, which is evaluated on the basis of the CO_2 avoided with respect to the benchmark (LNG or HFO) ship without onboard carbon capture (Fig. 6(a)). Due to its limited carbon capture rate, Case FG exhibits a cost of CO_2 avoided that is comparable (63.6–74.5 €/t for LNG ship, 100.2–104.4 €/t for HFO ship) to that of Case HP (74.7–83.6 €/t for LNG ship, 98.0–107.5 €/t for HFO ship). In turn, Case HP has a (much) lower cost of CO_2 avoided (−20% for LNG ship, -28% for HFO ship) with respect to Case FB (93.4–104.1 €/t for LNG ship, 136.1–149.1 €/t for HFO ship). This outcome substantiates the superior techno-economic performance of Case HP to the assessed alternatives.

4.3. Effect of carbon tax

This section provides a sensitivity analysis on the effect of accounting for a carbon tax on the ship CO_2 emissions over the total annual cost of both unabated (i.e., the baseline ship without onboard carbon capture) and abated solutions (i.e., the ship equipped with onboard carbon capture) (Fig. 7). The analysis is conducted on the most conservative scenario in terms of CO_2 unloading costs (i.e., S3). The intersections between the cost profiles of abated ships and their corresponding unabated baseline ship provide an estimate of the minimum value of carbon tax (i.e., the 'breakeven' carbon tax) that would make economically attractive the installation and operation of onboard carbon capture.

It emerges that Case FG and Case HP involve the lowest values of breakeven carbon tax, namely 75 and 84 €/t of CO_2 emitted (LNG ship), and 104 and 108 €/t of CO_2 emitted (HFO ship), respectively. Differently, the breakeven carbon tax for Case FB is equal to 104 €/t of CO_2 emitted (LNG ship) and 149 €/t of CO_2 emitted (HFO ship). However, if computing the cost of CO_2 avoided for these breakeven carbon tax thresholds, Case FG emerges as a penalised option due to its significant level of unabated CO_2 emissions, as it would involve 208.6 €/t of CO_2 avoided (LNG ship) and 334.4 €/t of CO_2 avoided (HFO ship). Differently, Case HP exhibits the best performance in terms of avoidance cost at breakeven carbon tax levels, with 102.2 €/t of CO_2 avoided (LNG ship) and 173.9 €/t of CO_2 avoided (HFO ship).

5. Conclusions

This article presented a techno-economic analysis of a post-combustion CO_2 capture system onboard an ultra-large container ship, running either on liquefied natural gas (LNG), or heavy fuel oil (HFO). Different plant designs were proposed depending on the energy source to cover the capture plant thermal and electric demands, namely a base configuration exploiting heat integration on the hot engine flue gases (Case FG), an alternative configuration based on a fuel-fired steam boiler (Case FB), and a novel system involving thermal integration with an electric heat pump (Case HP). It emerged that:

- Case FG can only achieve a partial carbon capture rate, namely 36.3% and 32.6% in the cases of LNG and HFO operation, respectively.
- HFO ship operation leads to a larger CO_2 flow rate to be separated than the LNG option. As a consequence, HFO-fed ships exhibit higher total annual costs for capture, on average +74% (Case FG), +72% (Case FB), and +35% (Case HP) with respect to their corresponding LNG alternative designs.

Table 6
Economic results: case studies, capital and operative expenditures, total annual costs, cost of CO_2 captured and avoided.

Case study		FG	FB	HP	FG	FB	HP
Ship fuel			LNG			HFO	
Flue gas heat		yes	yes	yes	yes	yes	yes
Steam boiler		no	yes	no	no	yes	no
Heat pump		no	no	yes	no	no	yes
CAPEX							
Absorber	[M€]	5.79	6.65	6.65	6.65	6.65	6.65
Stripper	[M€]	0.80	1.28	1.28	0.93	1.67	1.28
Reboiler	[M€]	0.47	0.94	0.95	0.54	1.23	0.99
Heat exchangers	[M€]	1.91	2.78	3.66	1.98	3.50	4.23
Compressors	[M€]	0.43	1.27	3.86	1.35	3.53	5.22
Onboard stor. tank (S1)	[M€]	1.64	4.09	4.09	2.07	5.63	4.51
Onboard stor. tank (S2)	[M€]	1.76	4.40	4.40	2.22	6.07	4.85
Onboard stor. tank (S3)	[M€]	3.65	9.12	9.12	4.61	12.57	10.06
Separators and others	[M€]	0.21	0.21	0.21	0.21	0.21	0.21
Total CAPEX (S1)	[M€]	11.25	17.22	20.72	13.74	22.42	23.10
Total CAPEX (S2)	[M€]	11.37	17.54	21.03	13.90	22.86	23.44
Total CAPEX (S3)	[M€]	13.26	22.26	25.75	16.28	29.36	28.64
fOPEX							
fOPEX (S1)	[M€/y]	0.34	0.52	0.62	0.41	0.67	0.69
fOPEX (S2)	[M€/y]	0.34	0.53	0.63	0.42	0.69	0.70
fOPEX (S3)	[M€/y]	0.40	0.67	0.77	0.49	0.88	0.86
vOPEX							
Excess fuel	[M€/y]	0.18	3.34	1.77	0.49	6.35	2.36
MEA solvent	[M€/y]	0.33	0.80	0.80	0.37	1.00	0.80
CO_2 trans. and stor. (S1)	[M€/y]	0.93	2.32	2.32	1.18	3.15	2.50
CO_2 trans. and stor. (S2)	[M€/y]	1.44	2.30	2.30	1.17	3.22	2.48
CO_2 trans. and stor. (S3)	[M€/y]	0.61	1.70	1.70	1.06	2.30	1.74
Reduced cargo loss (S1)	[M€/y]	0.21	0.72	0.74	2.02	2.95	2.69
Reduced cargo loss (S2)	[M€/y]	0.21	0.87	0.86	2.07	2.82	2.65
Reduced cargo loss (S3)	[M€/y]	0.78	1.79	1.72	2.05	4.48	3.82
Total vOPEX (S1)	[M€/y]	1.65	7.18	5.63	4.05	13.44	8.35
Total vOPEX (S2)	[M€/y]	2.16	7.32	5.74	4.10	13.38	8.29
Total vOPEX (S3)	[M€/y]	1.89	7.63	5.99	3.98	14.14	8.72
Total annual cost							
Total cost (S1)	[M€/y]	3.04	9.31	8.19	5.75	16.22	11.20
Total cost (S2)	[M€/y]	3.57	9.49	8.34	5.81	16.21	11.19
Total cost (S3)	[M€/y]	3.53	10.38	9.17	5.99	17.77	12.27
Cost of CO_2 capt. (S1)	[€/t]	62.2	77.4	68.0	93.8	97.8	84.8
Cost of CO_2 capt. (S2)	[€/t]	72.8	78.8	69.3	94.8	97.7	84.6
Cost of CO_2 capt. (S3)	[€/t]	72.1	86.2	76.2	97.7	107.1	92.8
Cost of CO_2 avoided (S1)	[€/t]	63.6	93.4	74.7	100.2	136.1	98.2
Cost of CO_2 avoided (S2)	[€/t]	74.5	95.1	76.0	101.3	136.0	98.0
Cost of CO_2 avoided (S3)	[€/t]	73.8	104.1	83.6	104.4	149.1	107.5

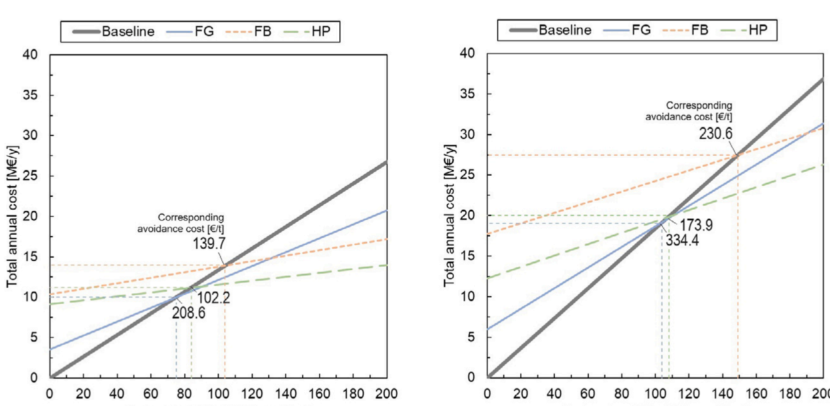

(a) LNG ship (b) HFO ship

Fig. 7. Sensitivity analysis of carbon tax [€/t of CO_2 emitted] over total annual cost [M€/y]: (a) LNG ship, and (b) HFO ship. Numbers labelled at intersections between cost lines represent the cost of CO_2 avoided [€/t of CO_2 avoided] computed for corresponding carbon tax.

- Storage tanks can be designed to be compatible with the volume available onboard the ship, but the increase in weight during navigation due to the progressively increasing amount of CO_2 to be stored onboard can result in significant costs. In fact, in the worst cases, the cost associated to the decrease in the available weight for cargo was found equal to 22%–35% of total annual costs, depending on LNG or HFO ship operation.
- As for CO_2 avoidance costs, Case FG sets at 63.6–74.5 €/t (LNG ship) and 100.2–104.4 €/t (HFO ship). Oppositely, Case HP exhibits a cost of CO_2 avoided of 74.7–83.6 €/t (LNG ship) and 98.0–107.5 €/t (HFO ship), while Case FB is always more expensive (93.4–104.1 €/t and 136.1–149.1 €/t for LNG and HFO ship operation, respectively).
- In the broader framework of encouraging emerging low-carbon technologies, if, for instance, a global carbon tax was accounted on CO_2 emissions, Case FG and Case HP would be cost effective with respect to the benchmark unabated ship for a value of taxation of about 75 or 104 €/t of CO_2 emitted depending on LNG or HFO ship operation. However, due to the partial carbon capture rate and limited performance in terms of CO_2 avoided of Case FG, Case HP was shown to exhibit the lowest CO_2 avoidance cost at breakeven carbon tax levels (102.2 and 173.9 €/t of CO_2 avoided for LNG and HFO ship operation, respectively).

Overall, the results highlight that the minimisation of additional (or excess) fuel consumptions is key when the aim is to achieve a substantial carbon capture rate (and carbon avoidance rate) while minimising parasitic emissions and specific capture (and avoidance) costs. As the flow rate of excess fuel depends on the energy production route (to cover capture, purification, and liquefaction demands), the implementation of an electric heat pump (Case HP) could be an efficient option to maximise the performance indicators of the onboard abatement system (e.g., CO_2 avoidance) at lower costs.

CRediT authorship contribution statement

Marco Visonà: Writing – review & editing, Methodology, Investigation, Formal analysis. **Fabrizio Bezzo:** Writing – review & editing, Supervision, Conceptualization. **Federico d'Amore:** Writing – review & editing, Writing – original draft, Supervision, Methodology, Investigation, Conceptualization.

Declaration of competing interest

The authors declare that they have no known competing financial interests or personal relationships that could have appeared to influence the work reported in this paper.

Data availability

Data will be made available on request.

Acknowledgements

This work has been supported under the National Recovery and Resilience Plan (NRRP), Mission 4 Component 2 Investment 1.4 - Call for tender No. 3138 of December 16, 2021 of the Italian Ministry of University and Research, funded by the European Union - NextGenerationEU [Award Number: CNMS named MOST, Concession Decree No. 1033 of June 17, 2022, adopted by the Italian Ministry of University and Research, CUP: C93C22002750006, Spoke 14 "Hydrogen and New Fuels"]. The authors would also like to thank Prof. M. Figari from Genova University (Italy) for the fruitful discussions on the design and operation of container ships.

Appendix A. Supplementary data

Supplementary material related to this article can be found online at https://doi.org/10.1016/j.cej.2024.149982.

References

[1] IEA, CO_2 emissions from international shipping in the net zero scenario, 2000–2030, 2023, https://www.iea.org/data-and-statistics/charts/co2-emissions-from-international-shipping-in-the-net-zero-scenario-2000-2030-3. (Accessed 30 November 2023).

[2] UNCTAD, UNCTAD review of maritime transport 2022, navigating stormy waters, 2022, https://unctad.org/rmt2022. (Accessed 30 November 2023).

[3] IMO, Fourth IMO greenhouse gas study, 2020, https://wwwcdn.imo.org/localresources/en/OurWork/Environment/Documents/Fourth%20IMO%20GHG%20Study%202020%20-%20Full%20report%20and%20annexes.pdf. (Accessed 30 November 2023).

[4] IMO, IMO strategy on reduction of GHG emissions from ships, 2023, https://wwwcdn.imo.org/localresources/en/OurWork/Environment/Documents/annex/MEPC%2080/Annex%2015.pdf. (Accessed 30 November 2023).

[5] R.H. Dolan, J.E. Anderson, T.J. Wallington, Outlook for ammonia as a sustainable transportation fuel, sustain, Energy Fuels 5 (2021) 4830–4841, http://dx.doi.org/10.1039/d1se00979f.

[6] J. Deng, X. Wang, Z. Wei, L. Wang, C. Wang, Z. Chen, A review of NOx and SOx emission reduction technologies for marine diesel engines and the potential evaluation of liquefied natural gas fuelled vessels, Sci. Total Environ. 766 (2021) 144319, http://dx.doi.org/10.1016/j.scitotenv.2020.144319.

[7] H. Xing, S. Spence, H. Chen, A comprehensive review on countermeasures for CO_2 emissions from ships, Renew. Sustain. Energy Rev. 134 (2020) 110222, http://dx.doi.org/10.1016/j.rser.2020.110222.

[8] F. d'Amore, A. Nava, P. Colbertaldo, Visconti M.C., C.G. Romano, Turning CO_2 from fuel combustion into e-fuel? Consider alternative pathways, Energy Convers. Manag. 289 (2023) 117170, http://dx.doi.org/10.1016/j.enconman.2023.117170.

[9] B. Stolz, M. Held, G. Georges, K. Boulouchos, Techno-economic analysis of renewable fuels for ships carrying bulk cargo in europe, Nat. Energy 7 (2022) 203–212, http://dx.doi.org/10.1038/s41560-021-00957-9.

[10] S. Lee, S. Yoo, H. Park, J. Ahn, D. Chang, Novel methodology for EEDI calculation considering onboard carbon capture and storage system, Int. J. Greenh. Gas Control 105 (2021) 103241, http://dx.doi.org/10.1016/j.ijggc.2020.103241.

[11] S. Cloete, A. Giuffrida, M.C. Romano, A. Zaabout, Heat pump-driven adsorption CO_2 capture for simple and cost-effective retrofits of coal power plants, Appl. Therm. Energy 236 (2024) 121456, http://dx.doi.org/10.1016/j.applthermaleng.2023.121456.

[12] S. Cloete, A. Giuffrida, M.C. Romano, A. Zaabout, Economic assessment of the swing adsorption reactor cluster for CO_2 capture from cement production, J. Clean. Prod. 275 (2020) 123024, http://dx.doi.org/10.1016/j.jclepro.2020.123024.

[13] S. Cloete, A. Giuffrida, M.C. Romano, A. Zaabout, The swing adsorption reactor cluster for post-combustion CO_2 capture from cement plants, J. Clean. Prod. 223 (2019) 692–703, http://dx.doi.org/10.1016/j.jclepro.2019.03.109.

[14] F. d'Amore, L.M.C. Pereira, S. Campanari, G. Matteo, M.C. Romano, A novel process for CO_2 capture from steam methane reformer with molten carbonate fuel cell, Int. J. Hydrogen Energy 48 (2023) 37366–37384, http://dx.doi.org/10.1016/j.ijhydene.2023.06.137.

[15] X. Luo, M. Wang, Study of solvent based carbon capture for cargo ships through process modelling and simulation, Appl. Energy 195 (2017) 402–413, http://dx.doi.org/10.1016/j.apenergy.2017.03.027.

[16] A. Awoyomi, K. Patchigolla, E.J. Anthony, Process and economic evaluation of an onboard capture system for LNG-fueled CO_2 carriers, Ind. Eng. Chem. Res. 59 (2020) 6951–6960, http://dx.doi.org/10.1021/acs.iecr.9b04659.

[17] M. Feenstra, J. Monteiro, J.T. van den Akker, M.R.M. Abu-Zahra, E. Gilling, E. Goetheer, Ship-based carbon capture onboard of diesel or LNG-fuelled ships, Int. J. Greenh. Gas Control 85 (2019) 1–10, http://dx.doi.org/10.1016/j.ijggc.2019.03.008.

[18] N.V.D. Long, D.Y. Lee, C. Kwag, Y.M. Lee, S.W. Lee, V. Hessel, M. Lee, Improvement of marine carbon capture onboard diesel fueled ships, Chem. Eng. Process. 168 (2021) 108535, http://dx.doi.org/10.1016/j.cep.2021.108535.

[19] J.A. Ros, E. Skylogianni, V. Doedée, J.T. van den Akker, A.W. Vredeveldt, M.J.G. Linders, E.L.V. Goetheer, J.G.M.S. Monteiro, Advancements in ship-based carbon capture technology on board of LNG-fuelled ships, Int. J. Greenh. Gas Control 114 (2022) 103575, http://dx.doi.org/10.1016/j.ijggc.2021.103575.

[20] C. Ji, S. Yuan, M. Huffman, M.M. El-Halwagi, Q. Wang, Post-combustion carbon capture for tank to propeller via process modeling and simulation, J. CO_2 Util. 51 (2021) 101655, http://dx.doi.org/10.1016/j.jcou.2021.101655.

[21] Mærsk, The role of onboard carbon capture in maritime decarbonization, 2022, https://cms.zerocarbonshipping.com/media/uploads/publications/The-role-of-onboard-carbon-capture-in-martime-decarbonization.pdf. (Accessed 30 November 2023).

[22] OGCI, Is carbon capture on ships feasible?, 2021, https://www.ogci.com/wp-content/uploads/2023/04/OGCI_STENA_MCC_November_2021.pdf. (Accessed 30 November 2023).

[23] A. Einbu, T. Pettersen, J.A. Morud, C.K. Tobiesen, R. Jayarathna, G. Nysæther Skagestad, Energy assessments of onboard CO_2 capture from ship engines by MEA-based post combustion capture system with flue gas heat integration, Int. J. Greenh. Gas Control 113 (2022) 103526, http://dx.doi.org/10.1016/j.ijggc.2021.103526.

[24] V. Negri, M.A. Charalambous, J.D. Medrano-García, G. Guillén-Gosálbez, Navigating within the safe operating space with carbon capture on-board, ACS Sustain. Chem. Eng. 10 (2022) 17134–17142, http://dx.doi.org/10.1021/acssuschemeng.2c04627.

[25] L.S. Tan, A.M. Shariff, K.K. Lau, M.A. Bustam, Factors affecting CO_2 absorption efficiency in packed columns: A review, J. Ind. Eng. Chem. 18 (2012) 1874–1883, http://dx.doi.org/10.1016/j.jiec.2012.05.013.

[26] E.O. Agbonghae, K.J. Hughes, D.B. Ingham, L. Ma, M. Pourkashanian, Optimal process design of commercial-scale amine-based CO_2 capture plants, Ind. Eng. Chem. Res. 53 (2014) 14815–14829, http://dx.doi.org/10.1021/ie5023767.

[27] A.H. Hassan, J.M. Corberán, M. Ramirez, F. Trebilcock-Kelly, J. Payá, A high-temperature heat pump for compressed heat energy storage applications: Design, modeling, and performance, Energ. Rep. 8 (2022) 10833–10848, http://dx.doi.org/10.1016/j.egyr.2022.08.201.

[28] H. Deng, S. Roussanaly, G. Skaugen, Techno-economic analyses of CO_2 liquefaction: Impact of product pressure and impurities, Int. J. Refrig. 103 (2019) 301–315, http://dx.doi.org/10.1016/j.ijrefrig.2019.04.011.

[29] P.A. Brownsort, Briefing on carbon dioxide specifications for transport, 1st report of the thematic working group on: CO_2 transport, storage and networks, in: CCUS Project Networks, 2019, https://www.ccusnetwork.eu/sites/default/files/TG3_Briefing-CO2-Specifications-for-Transport.pdf. (Accessed 30 November 2023).

[30] S. Roussanaly, H. Deng, G. Skaugen, T. Gundersen, At what pressure shall CO_2 Be transported by ship? An in-depth cost comparison of 7 and 15 barg shipping, Energies 14 (2021) 5635, http://dx.doi.org/10.3390/en14185635.

[31] G.P. Towler, R.K. Sinnott, Chemical Engineering Design: Principles, Practice and Economics of Plant and Process Design, second ed., Butterworth-Heinemann, 2008.

[32] NETL, Process equipment cost estimation final report, 2002, https://www.osti.gov/servlets/purl/797810.

[33] W.E. Hand, From flow sheet to cost estimate, Petrol. Refiner. 37 (1958) 331–334.

[34] H.M. Kvamsdal, S. Ehlers, A. Kather, P. Khakharia, M. Nienoord, P.L. Fosbøl, Optimizing integrated reference cases in the OCTAVIUS project, Int. J. Greenh. Gas Control 50 (2016) 23–36, http://dx.doi.org/10.1016/j.ijggc.2016.04.012.

[35] Ship, Bunker, Global average bunker prices, 2023, https://shipandbunker.com/prices/av/global/av-g20-global-20-ports-average. (Accessed 30 November 2023).

[36] IPCC, Special report on carbon dioxide capture and storage, 2005, https://www.ipcc.ch/site/assets/uploads/2018/03/srccs_wholereport-1.pdf. (Accessed 30 November 2023).

[37] IEA, Indicative CO_2 storage cost curve for the United States, onshore, 2020, https://www.iea.org/data-and-statistics/charts/indicative-co2-storage-cost-curve-for-the-united-states-onshore. (Accessed 30 November 2023).

[38] F. d'Amore, M.C. Romano, F. Bezzo, Optimal design of European supply chains for carbon capture and storage from industrial emission sources including pipe and ship transport, Int. J. Greenh. Gas Control 109 (2021) 103372, http://dx.doi.org/10.1016/j.ijggc.2021.103372.

[39] Drewry, World container index, 2023, https://en.macromicro.me/charts/44756/drewry-world-container-index. (Accessed 30 November 2023).